Programmable Patterning of Polymeric Microparticles By Floating Electrodes-Assisted Electrospray

Xu Zhang and Yi Zhao*

Laboratory for Biomedical Microsystems

Department of Biomedical Engineering, The Ohio State University

Abstract

We introduce an innovative method for patterning one or multiple types of polymeric microparticles by electrospraying them towards a collecting surface patterned with an array of microelectrodes. By independently programming the electric state of each microelectrode, microparticles can be confined within desired regions with a high patterning contrast. The patterning principle and the role of the floating electrodes are discussed. Co-patterning of multiple types of particles on a planar surface and along the vertical direction is demonstrated. With the superior co-patterning capacity and the simple configuration, this work is expected to facilitate the development of biosensing, microscale tissue engineering and other microparticle-based total analysis.

*To whom all correspondence should be addressed.
Yi Zhao, Ph.D.
Rm 294 Bevis Hall, 1080 carmack Road
Columbus, OH 43210, USA
Tel: (614) 247-7424
Fax: (614) 292-7301

1. Introduction

Spatial patterning of micro/nanoscale particulate species has become increasingly popular due to the broad applications in chemical and biological engineering [1, 2]. For example, assembly of colloidal microparticles plays a crucial role in electrical resistive chemical and biosensors [3]; surface patterned microparticles can be used to regulate cell attachment [4] as well as to study the effect of topographical cues on live cells [5]. Current approaches utilize electrostatic force [6], physical confinement [7], capillary force [8], or dielectrophoresis [9] for positioning colloidal microparticles at desired spatial sites. Among these methods, electrostatic manipulation of particles is attractive due to the enhanced surface-to-volume ratio at the small scales [10-12]. For example, aerosol droplets containing small particles was selectively deposited on prepatterned electrodes [13, 14], where the patterning resolution can be enhanced by introducing ions and utilizing the "electrostatic lens" [15]. In these electrostatic patterning studies, surface distribution of the electric charges is often controlled using conductive electrodes, chemically modifying the surface [6]; coating a layer of surfactant [10]; or transferring the charge from a PDMS stamp [16, 17]. The electrostatic interaction between the incoming particles and the charged collecting surface preferentially attracts the particles to the patterned regions. Patterning of multiple types of particles is primarily based on the difference in affinity conditions [11]. However, the complexity of surface modification for co-patterning increases with the number of particle type. In addition, the particle co-patterning along the vertical dimension is not demonstrated. This, to a certain extent, compromises the efficacy of electrostatic particle patterning in comprehensive

biochemical analyses where co-patterning of two or multiple types of particulate species is required.

In this technical note, we demonstrate microparticle patterning by electrospraying polymer on a micropatterned collecting surface, where the high DC voltage bias turns the positively charged polymer solution into a stream of polymer droplets and drag these droplets towards desired regions. The electric connection states of individual microelectrodes on the collecting surface are programmed to spatially confine the microparticles. In particular, the floating electrodes are used to enhance the patterning contrast, which allow co-patterning of multiple types of microparticles on the planar surface or along the vertical direction.

2. Patterning of A Single Type of Microparticles

Microparticle patterning was demonstrated by using a non-toxic biodegradable polymer polycaprolactone (PCL) (Sigma-Aldrich, Mn=60,000). The polymer solution was prepared by mixing 10wt% PCL with acetone. In the electrospray process, a DC voltage bias of 20kV was applied while the PCL solution was pumped through a metallic capillary at a flow rate of 0.5ml/hr. Under the electrostatic field, the PCL droplet at the capillary tip deformed into a conical shape. When the electrorepulsive force overcame the surface tension, a liquid jet was ejected, forming a stream of small and highly charged liquid droplets. The solvent in the droplets evaporated while the droplets flew towards the collecting surface that was positioned at 15cm vertical distance from the capillary tip. PCL microparticles thus formed as the solvent evaporated, and eventually deposited on the collecting surface consisting of an array

of interdigitated conductive microelectrodes. Electrospray was performed for 30 seconds while all the electrodes were connected to the ground. The results showed that most microparticles were deposited on the grounded electrode surface (Figure 1a). The particles density in the electrode area was significantly higher than that in the dielectric inter-electrode area. By taking the particle density in the ground electrode as the reference, the particle density in the inter-electrode area was about 31% (Figure 1c).

Electrospray was also performed by dividing the microelectrodes into two electric connection groups. The odd numbered electrodes were grounded while the even numbered electrodes were floated from the ground level. After 30 second electrospray most microparticles were deposited on the ground electrodes, while very few particles were observed on the floating electrodes and the inter-electrode area (Figure 1b). The enhancement of the patterning contrast was also observed: the normalized particle density in the inter-electrode area reduced to less than 16%. The particle density on the floating electrodes was even lower (7%) (Figure 1c). Under both conditions (with and without the floating electrodes), the particle sizes had a normal distribution with the peak around 3μm in diameter. These results were concluded that the collecting substrate with microelectrodes can pattern small particles; while the floating electrodes can enhance the patterning contrast. This is especially important for patterning particles with the size of a few microns or larger where the efficacy of electrostatic focusing is compromised due to their relatively smaller surface-to-volume ratio comparing to that of nanoparticles.

According to previous studies, the size of liquid droplets is determined by the electrospray parameters, as expressed by [21]:

$$R \propto \left(\rho v_F^2 \gamma\right)^{1/3} \tag{1}$$

where ρ stands for the liquid density, v_F stands for liquid flow rate and γ stands for surface tension of the droplet at the capillary tip. The droplet size is dominantly controlled by the liquid flow rate and secondly by the applied voltage [22], while the electrode configuration does not affect the droplet size. Therefore, the droplet dynamics can be determined using the following equation [18-20]:

$$m_i \frac{d\vec{u}_i}{dt} = q_i \vec{E} + D\frac{\pi d_i^2 \rho\left(\vec{u}_f - \vec{u}_i\right)\cdot\left|\vec{u}_f - \vec{u}_i\right|}{8} + \sum_{i\neq j}^{N} \frac{q_i q_j}{4\pi\varepsilon_0 r_{i,j}^3}\vec{r}_{i,j} \tag{2}$$

where D is the drag coefficient, E is the electric field strength, m is the droplet mass, q is droplet charge, d is the droplet diameter, $r_{i,j}$ is the distance between two droplets, t is the time, u_i is the droplet velocity, u_f is the air flow velocity, ε_0 is the permittivity of free space, and ρ is the air density. It is assumed that with a fast evaporating solvent the droplet size and mass are determined within the very beginning period after the ejection, and keep largely unchanged during the subsequent flight towards the collecting substrate.

The spatial patterning of microparticles is due to the non-uniform electric field caused by the microelectrodes, which can be understood by examining the profile of the electric potential wells in the region close to the collecting surface. Finite element analysis showed that when all the microelectrodes are grounded (denoted by red block), a potential well forms above each microelectrode (Figure 2a). The depth of the potential well is a function of the vertical distance to the collecting substrate, the voltage bias, and the electrospray distance. The

motion of the positively charged microparticles is governed by the initial particle momentum, the drag force by air, and the electrostatic force applied by the potential well. For small particles with high surface-to-volume ratio, the electrostatic force dominates. The particles are thus attracted to the conductive surface of the microelectrodes where the minimal potential occurs. Given the voltage bias and the electrospray distance used in this case, the potential well depth of an electrode with 200μm in width and 600μm in spacing is about 5V on the collecting surface. When a floating electrode (denoted by green block) is positioned between two neighboring ground electrodes, the local electric field is altered. Because the floating electrode is not electrically connected, its initial potential is indefinite. The floating electrode experiences a capacitive coupling with the local field determined by all the adjacent electrodes with definite voltages. For instance, the capacitance between a coupled electrodes pair is given by [23]:

$$C = \frac{\oint_{S_1} \varepsilon_0 \vec{E} \cdot d\vec{a}}{\int_{(1)}^{(2)} \vec{E} \cdot d\vec{s}} \tag{3}$$

Where *S and a* denotes the electrode area, *s* is the distance between two electrodes, number 1 and 2 denotes the ground electrode and the floating electrode respectively. The capacitance *C* between the two electrodes is defined as the ratio of electric charges on the ground electrode to the voltage between the two electrodes. Because there is no electrical charge transfer between the two electrodes in a pair, the net charge on the floating electrode is zero [24]. Therefore, a numerical method must be applied to integrate the Laplace equation $\nabla^2\varphi = 0$ with proper boundary conditions [25], where φ denotes the electrical potential. The

equilibrium depth of the potential well in presence of the floating electrode was thus determined numerically, as about 8V (Figure 2b).

As the figure shows, the increase of the potential well depth upon the addition of a floating electrode leads to a steeper sidewall of the potential well. This suggested that in presence of floating electrodes a positively charged microparticle may experience a larger electrostatic force than that without floating electrodes while at the same vertical distance from the collecting substrate. In other words, the floating electrodes provide an extra force to push the microparticles towards the ground electrodes (or away from themselves). This was further validated by simulating the particle trajectory in the region with a non-uniform electric field due to the addition of floating electrodes. A total of 100 microparticles with the size and velocity determined by equations (1)&(2) are uniformly distributed along the horizontal plane and enter the near-electrode region from the top boundary (Figure 2c) The results showed that the all particles were repelled by the floating electrodes and deposited on ground electrodes, confirming the presence of the electric potential wells. The addition of floating electrodes is especially useful for patterning large particles. Experiments confirmed that relatively large particles gathered around the ground electrodes in presence of floating electrodes (Figure 1b), while they widely spread on the substrate without the floating electrodes (Figure 1a).

3. Co-patterning of Multiple Types of Microparticles

One beauty of using floating electrodes is to enable programmable patterning of multiple types of microparticles on a single collecting substrate. Co-patterning of two types of

microparticles was demonstrated (Figure 3). Each electrode was individually switchable between the grounded state (when it served as the target of patterning) and the floating state (when it served to enhance the patterning contrast). In the experiment, the electrodes on the left and on the right were first grounded; while the electrode in the middle was floating. PCL microparticles Type I (mixed with the fluorescence dye Rhodamine B (Ex/Em: 540nm/625nm)) were sprayed on the substrate for 90 seconds. Afterwards, the electrodes on the left and right were set to be floating; and the electrode in the middle was grounded. PCL microparticles Type II (mixed with the fluorescence dye Calcein blue (Ex/Em: 370nm/435nm)) were sprayed for another 90 seconds. Microscopic observation showed that microparticles Type I were confined within the two electrodes on the sides, while microparticles Type II were confined within the middle electrode.

Besides planar co-patterning, this method can also pattern multiple types of microparticles along the third dimension. To demonstrate this, microparticles Types II and I were first patterned on the left and right electrodes respectively, following the same procedure as above mentioned. Afterwards, microparticles Type I were patterned on the left electrode on top of the first layer made up of microparticles Type II. Similarly, microparticles Type II were patterned on the right electrode on top of the first layer made up of micropartciles Type I. The total thickness of the microparticle assembly on each electrode was about 85μm. The vertical arrangement of microparticles was examined using fluorescence confocal microscopy: at the vertical distance of 25μm from the collecting substrate, most microparticles on the left electrode belonged to Type II, while most microparticles on the right electrode belonged to

Type I. The compositions on the two electrodes changed gradually as the focal plane moved away from the collecting substrate vertically. At the distance of 60μm away from the collecting substrate, the particle compositions on the two electrodes switched, as indicated by the color change (Figure 4). Collectively, multiple types of microparticles can be co-patterned on the lateral plane or along the third dimension by programming the electric connection states of the microelectrodes. The patterning complexity does not change drastically with the increasing number of the particle type, thus making it easier to perform chemical and biomolecular analysis with heterogeneous patterning, particularly allowing co-culturing of multiple types of cells to form a functional engineered tissue.

4. Conclusion

A floating electrode-assisted electrospray method for the production of micropatterns made up of one or more types of microparticles has been presented. This method creates a spatially heterogeneous electric potential field to pattern microparticles within desired regions. The floating electrodes increase the depth of electric potential wells and thus enhance the patterning contrast, allowing patterning of particles in the microscale. Moreover, co-patterning of two or more types of microparticles within the lateral plane as well as along the vertical direction is made possible by programming the electric connection states of the electrodes. Comparing the previous microparticle patterning technologies, temporal and spatial programming of the electric field presented in this technical note greatly simplifies the micropatterning process, especially for patterning multiple types of particles. The co-patterning capacity is thus extended, which is expected to facilitate microscale tissue

engineering and micro-total-analysis especially when multiple particulate species and/or biomolecular entities need to be involved.

Acknowledgment

This work was partially supported by Institute for Materials Research at the Ohio State University.

Figure Captions

Figure 1: Spatial distribution of microparticles after a 30-second electrospray. (a) All the electrodes were connected to the ground; (b) The electrode on the right was grounded while the one on the left was floating; (c) Normalized particle density in different regions of the collecting surface. The black bar denotes the result with the electric connection state (a). The shadowed bar denotes the result with the electric connection state (b). Data were recorded from 6 independent samples and were represented as mean±SD. **P<0.01 for a comparison of particles depositing in the inter-electrode region to those in the ground electrode region. Scale bar=500μm.

Figure 2: Finite element analysis of the electric potential profile and the particle trajectory in the close vicinity to the micropatterned electrodes during an electrospray process. (a) Profile of the electric potential at the collecting surface when all the electrodes were grounded; (b) Profile of the electric potential at the collecting surface when floating electrodes were positioned between the neighboring ground electrodes. (c) Particle trajectory with the electrode configuration in (b), where the particle mass is estimated as 3.6^{-14}kg, charge per particle is estimated as 3.84^{-15}C. The red blocks denote the ground electrodes. The green blocks denote the floating electrodes.

Figure 3: Fluorescence micrographs showing the programmable patterning on a planar collecting surface. (a) Electrodes array used for microparticle patterning; (b) When the electrodes on the left and right sides were grounded and the one in the middle was floating,

Type I particles (red) were deposited primarily on the two electrodes on the sides; (c) When the electrode in the middle was grounded while the two on the sides were floating, Type II particles (blue) were confined within the middle electrode; (d) Overlapped fluorescence image showing the co-patterning of the two types of microparticles. The arrows denote the location of floating electrodes. Scale bar=500μm.

Figure 4: Fluorescence confocal micrograph shows the multilayer programmable patterning with two types of microparticles. (a) The electrodes used for the multilayer patterning; (b) (Upper panel) Fluorescence image by wide field fluorescence microscopy where emission throughout the entire thickness is included. (Middle panel) Overlapped confocal images from two emission wavelengths at a bottom layer (Z=25μm) of the microparticle assembly. Microparticles on the left electrode primarily belonged to Type II (blue), while those on the right electrode primarily belonged to Type I (red). (Bottom panel) Overlapped confocal images from two emission wavelengths at a top layer (Z=60μm) of the microparticle assembly. Microparticles on the left electrode primarily belonged to Type I, while those on the right electrode primarily belonged to Type II. Scale bar=500μm.

References

[1] A.N. Shipway, E. Katz, I. Willner, Chemphyschem, 1 (2000) 18-52.

[2] F.L. Yap, Y. Zhang, Biosens Bioelectron, 22 (2007) 775-788.

[3] O.D. Velev, E.W. Kaler, Langmuir, 15 (1999) 3693-3698.

[4] X. Li, G. Koller, J. Huang, L. Di Silvio, T. Renton, M. Esat, W. Bonfield, M. Edirisinghe, J R Soc Interface, 7 (2010) 189-197.

[5] N.J. Gleason, C.J. Nodes, E.M. Higham, N. Guckert, I.A. Aksay, J.E. Schwarzbauer, J.D. Carbeck, Langmuir, 19 (2003) 513-518.

[6] J. Aizenberg, P.V. Braun, P. Wiltzius, Physical Review Letters, 84 (2000) 2997-3000.

[7] D.Y. Xia, A. Biswas, D. Li, S.R.J. Brueck, Adv Mater, 16 (2004) 1427-1432.

[8] Y. Cui, M.T. Bjork, J.A. Liddle, C. Sonnichsen, B. Boussert, A.P. Alivisatos, Nano Lett, 4 (2004) 1093-1098.

[9] A. Docoslis, P. Alexandridis, Electrophoresis, 23 (2002) 2174-2183.

[10] K.M. Chen, X.P. Jiang, L.C. Kimerling, P.T. Hammond, Langmuir, 16 (2000) 7825-7834.

[11] H.P. Zheng, I. Lee, M.F. Rubner, P.T. Hammond, Adv Mater, 14 (2002) 569-572.

[12] P.T. Hammond, in: F. Caruso (Ed.) Colloids and Colloid Assemblies: Synthesis, Modification, Organization and Utilization of Colloid Particles, Wiley-VCH, Weihem, 2004.

[13] W. Prost, F.E. Kruis, F. Otten, K. Nielsch, B. Rellinghaus, U. Auer, A. Peled, E.F. Wassermann, H. Fissan, F.J. Tegude, Microelectron Eng, 42 (1998) 535-538.

[14] F. Otten, U. Auer, F.E. Kruis, W. Prost, F.J. Tegude, H. Fissan, Mater Sci Tech-Lond, 18 (2002) 717-720.

[15] H. Kim, J. Kim, H.J. Yang, J. Suh, T. Kim, B.W. Han, S. Kim, D.S. Kim, P.V. Pikhitsa, M. Choi, Nat Nanotechnol, 1 (2006) 117-121.

[16] T.J. Krinke, K. Deppert, M.H. Magnusson, H. Fissan, Part Part Syst Char, 19 (2002) 321-326.

[17] M. Kang, H. Kim, B.W. Han, J. Suh, J. Park, M. Choi, Microelectron Eng, 71 (2004) 229-236.

[18] J.C.L. A.M. Ganan-Calvo, J. Davila, A. Barrero, , J. Aerosol Sci 25 (1994) 1121-1142.

[19] K. Tang, A. Gomez, Phys Fluids, 6 (1994) 2317-2332.

[20] R.P.A. Hartman, J.P. Borra, D.J. Brunner, J.C.M. Marijnissen, B. Scarlett, J Electrostat, 47 (1999) 143-170.

[21] O.V. Salata, Curr Nanosci, 1 (2005) 25-33.

[22] K.Q. Tang, A. Gomez, J Colloid Interf Sci, 184 (1996) 500-511.

[23] J.R.M. H. A. Haus, Electromagnetic Fields and Energy, Prentice-Hall International, Englewood Cliffs, 1989.

[24] S. Golan, D. Elata, M. Orenstein, U. Dinnar, Electrophoresis, 27 (2006) 4919-4926.

[25] M. Keddam, X.R. Novoa, V. Vivier, Corros Sci, 51 (2009) 1795-1801.

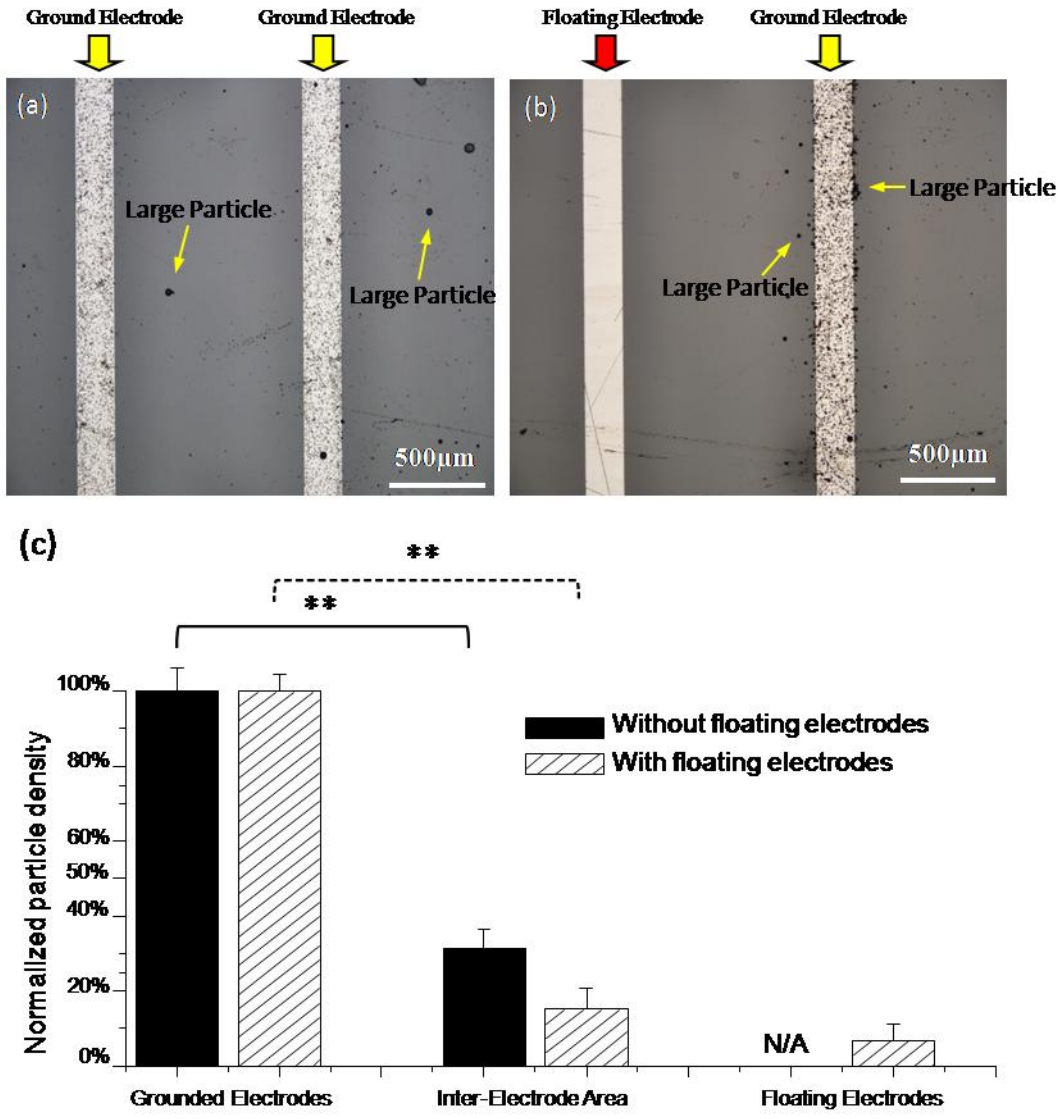
Ground Electrode
Ground Electrode
Floating Electrode
Ground Electrode
(a)
Large Particle
Large Particle
500µm
(b)
Large Particle
Large Particle
500µm
(c)
**
**
100%
80%
60%
50%
40%
20%
0%
Normalized particle density
Without floating electrodes
With floating electrodes
N/A
Grounded Electrodes
Inter-Electrode Area
Floating Electrodes

Figure 1

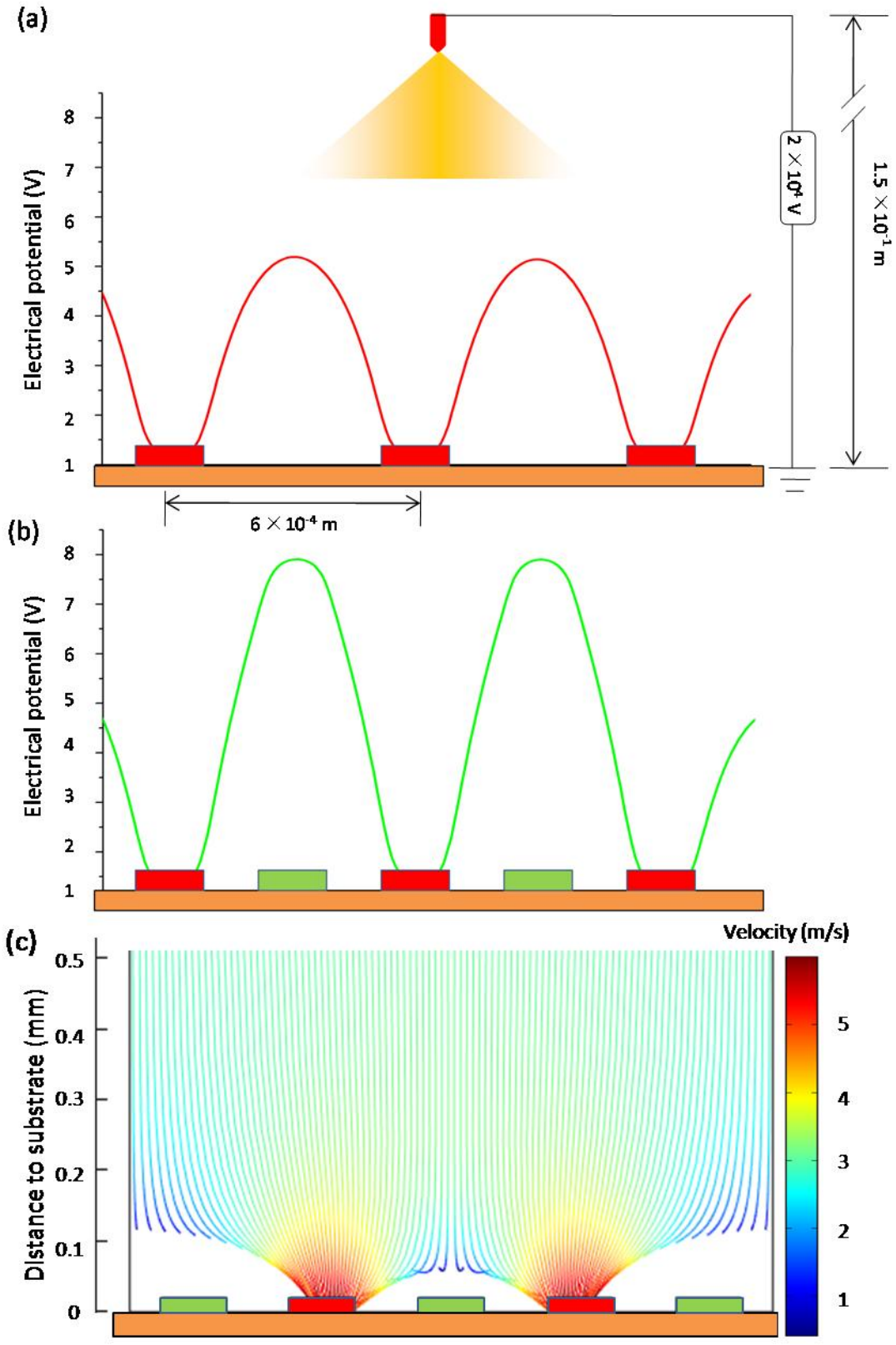
(a)
Electrical potential (V)
8
7
6
5
4
3
2
1
2 × 10⁴ V
1.5 × 10⁻¹ m
6 × 10⁻⁴ m
(b)
Electrical potential (V)
8
7
6
5
4
3
2
1
(c)
Velocity (m/s)
Distance to substrate (mm)
0.5
0.4
0.3
0.2
0.1
0
5
4
3
2
1

Figure 2

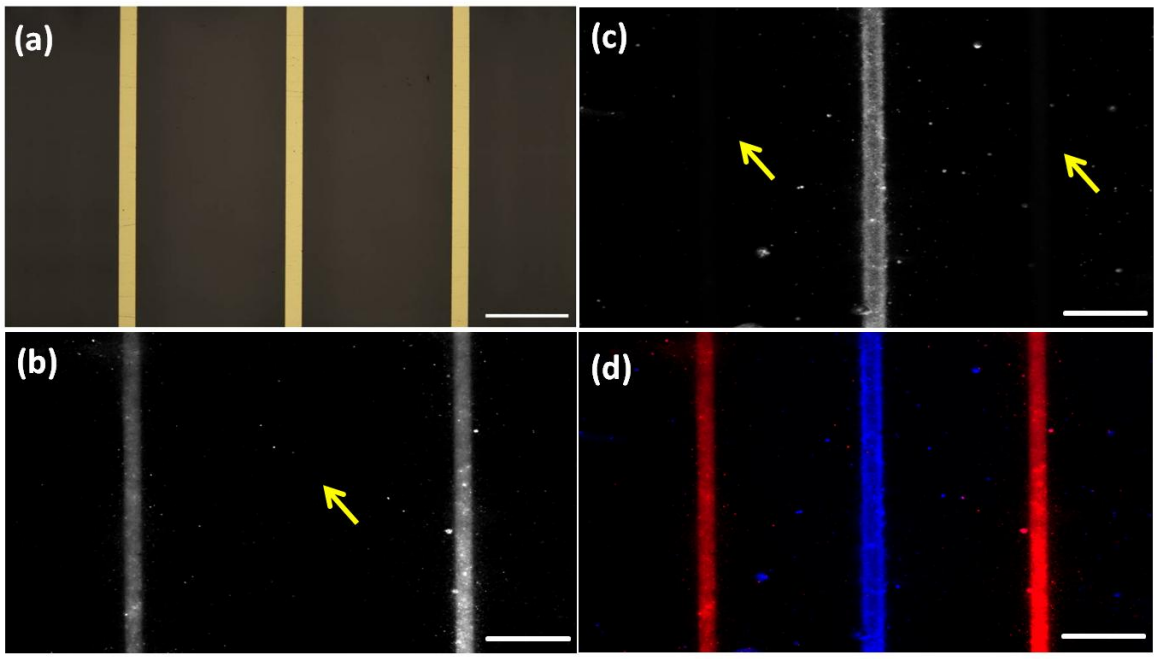

Figure 3

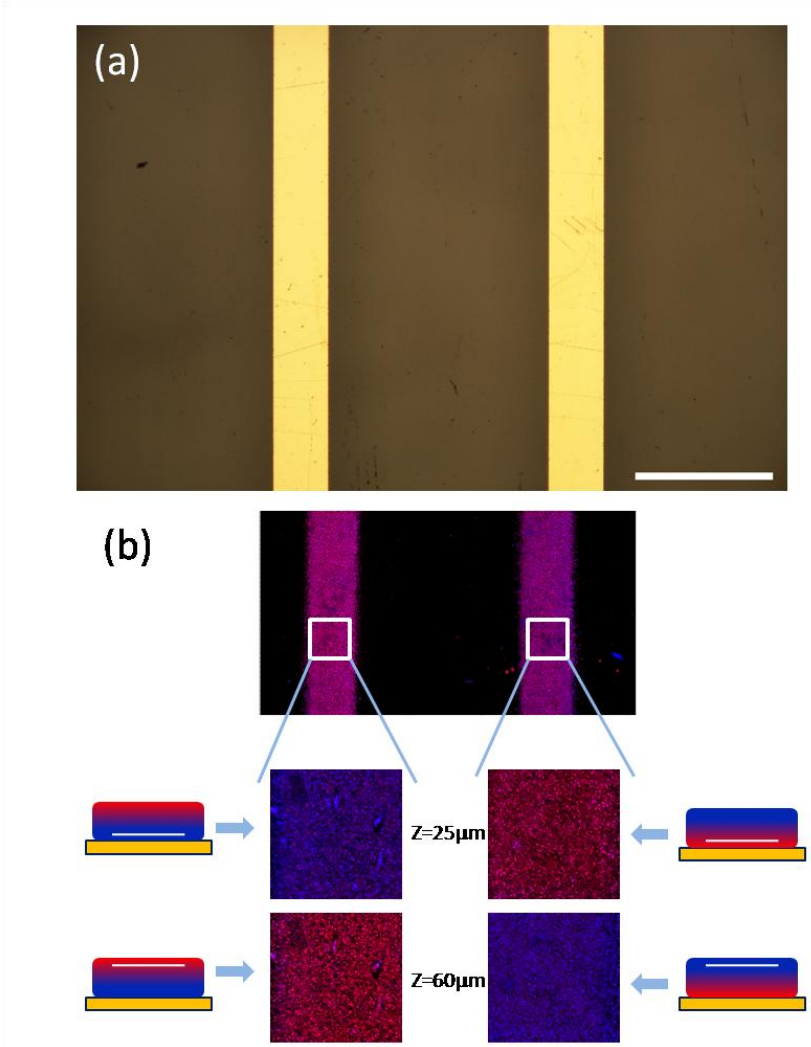

Figure 4